

RESEARCH

Open Access



# CAP1: a novel extracellular vesicle marker linked to endothelial senescence in atherosclerosis

Ignacio Hernandez<sup>1,4</sup>, Laura Botana<sup>3</sup>, Javier Diez-Mata<sup>1</sup>, Laura Tesoro<sup>1,4</sup>, Beatriz Jimenez-Guirado<sup>1</sup>, Claudia Gonzalez-Cucharero<sup>1</sup>, Nunzio Alcharani<sup>1</sup>, Jose Luis Zamorano<sup>2,5</sup>, Marta Saura<sup>2,6</sup> and Carlos Zaragoza<sup>1,4\*</sup>

## Abstract

Endothelial senescence (ES) contributes to aging-related disorders and triggers a senescence-associated secretory-pattern (SASP), releasing Extracellular Vesicles (EVs), potentially impacting atherosclerosis. We used EVs from young (8 weeks) and aged (24 months) ApoE-knockout mice to detect ES in human aortic (HAEC) and coronary (CAEC) endothelial cells. Age-related atherosclerosis was confirmed by increased atheroma plaque formation in aged compared to young ApoE-knockout mice fed a high-fat diet, and the contribution of EVs from aged ApoE-knockout mice on ES was evidenced by a replicative senescence assay in cultured HAEC and CAEC, starting with the promotion of ES. A proteomic analysis depicted the recently PCSK9-associated CAP1 protein as a cargo component in EVs from aged animals and highly expressed in mouse and human endarterectomy plaques. Gene silencing of CAP1 inhibited HAEC and CAEC ES while overexpressing CAP1 in these cells restored the senescent-phenotype. The in vivo contribution of CAP1 was assessed by injecting CAP1-containing EVs isolated from aged ApoE-knockout mice into wild-type (WT) mice fed either a regular or high-fat diet. Compared to the EVs from young mice, the CAP1-containing EVs led to a pronounced ES along with the formation of intraluminal atheroma plaques. Similarly, young ApoE-knockout mice developed thickened and calcified atheroma plaques, along with increased  $\beta$ -Gal-positive aortic staining when injected with EVs isolated from aged ApoE-knockout mice, like the atheroma plaques observed in aged ApoE-knockout animals. In conclusion, early molecular targets of ES may contribute to better management of atherosclerosis, in which here we unveiled CAP1 as a new molecular target.

**Keywords** Atherosclerosis, Cyclase associated protein-1 (CAP1), Endothelial senescence, Extracellular vesicles

\*Correspondence:

Carlos Zaragoza  
c.zaragoza.prof@ufv.es

<sup>1</sup>Unidad Mixta de Investigación Cardiovascular Universidad Francisco de Vitoria Hospital Ramon y Cajal (IRYCIS), Madrid, Spain

<sup>2</sup>Centro de Investigación Biomédica en Red de Enfermedades Cardiovasculares (CIBERCV), Instituto de Salud Carlos III (ISCIII), Madrid, Spain

<sup>3</sup>Facultad de Ciencias Experimentales, Universidad Francisco de Vitoria, Madrid, Spain

<sup>4</sup>Facultad de Medicina, Universidad Francisco de Vitoria, Madrid, Spain

<sup>5</sup>Departamento de Cardiología, Hospital Universitario Ramón y Cajal (IRYCIS), Madrid, Spain

<sup>6</sup>Unidad de Fisiología, Departamento de Biología de Sistemas, Universidad de Alcalá (IRYCIS), Alcalá de Henares, Madrid, Spain



© The Author(s) 2025. **Open Access** This article is licensed under a Creative Commons Attribution-NonCommercial-NoDerivatives 4.0 International License, which permits any non-commercial use, sharing, distribution and reproduction in any medium or format, as long as you give appropriate credit to the original author(s) and the source, provide a link to the Creative Commons licence, and indicate if you modified the licensed material. You do not have permission under this licence to share adapted material derived from this article or parts of it. The images or other third party material in this article are included in the article's Creative Commons licence, unless indicated otherwise in a credit line to the material. If material is not included in the article's Creative Commons licence and your intended use is not permitted by statutory regulation or exceeds the permitted use, you will need to obtain permission directly from the copyright holder. To view a copy of this licence, visit <http://creativecommons.org/licenses/by-nc-nd/4.0/>.

## Introduction

Endothelial dysfunction (ED) is recognized as a critical underlying condition of cardiovascular disease [1], in which about one-third affects those under the age of 70. Endothelial senescence (ES) is an aging-related response and a leading cause of ED by still unknown mechanisms. Our understanding of the misalignment between chronological and vascular aging must still be completed in this context. Establishing a distinct molecular signature of senescence can enhance our comprehension and potentially prevent vascular aging-related cardiovascular disease influencing ED [2], a primary etiological source of atherosclerosis.

Cellular senescence represents a programmed stress response that initiates a lasting cell cycle arrest and activates the senescence-associated secretory phenotype (SASP), encompassing the release of various types of Extracellular Vesicles (EVs) [3, 4]. Endothelium-derived EVs are surrogate markers of endothelial injury [5], released in age-related CVD, including atherosclerosis and acute coronary syndrome [6]. Likewise, recent findings have shown that EV release induces endothelial senescence-related ED [7]. Hence, an effort to understand ES involves accurately defining the cargo in EVs to prevent senescence-related ED.

Cyclase-associated protein 1 (CAP1) is an actin filament capping protein that regulates actin cytoskeleton dynamics [8]. Hence, CAP1 plays a role in cell migration and invasion, processes that are essential in various physiological and pathological contexts, including atherosclerosis. CAP1 has emerged as a novel regulator of cholesterol metabolism by interacting with PCSK9, thereby modulating the progression of atherosclerosis [9].

In this study, we have undertaken a comprehensive analysis of the cargo within EVs released by young and aged atherosclerotic mice to shed light on ES mechanisms underlying vascular aging. Notably, our findings reveal, for the first time, the role of CAP1 as a novel predictive marker for early aging signals derived from EVs in atherosclerosis.

## Materials and methods

### Reagents and equipment

CAP1 (ab155079, 1:1000), PCSK9 (ab181142, 1:1000),  $\beta$ -Tubulin (ab6046, 1:2000), GAPDH (ab22555, 1:2000), Goat anti-mouse IgG (AB97019, 1:2000), Goat anti-rabbit IgG (AB6721, 1:2000) and Senescence Detection Kit (ab65351) were from Abcam (Cambridge, UK). Oil Red O (#O0625-25G), Hematoxylin (#253949.1211), Eosin (#56879.1210), and BAY11-7083 (#196870) inhibitor of NF $\kappa$ B activation, were from Merck Millipore (Burlington, Massachusetts, USA). Opti-MEM Reduced Serum Medium (Cat. 31985047), Lipofectamine RNAiMAX

transfection reagent (Cat. 13778100) Human CAP1 Silencer Select siRNA (Cat. AM16708) was from Life Technologies (Carlsbad, CA, USA). Evolocumab was from AMGEN (Amgen, Barcelona, SPAIN). Line Human Aortic Endothelial Cells (HAEC, #6100) was from Science Cell (Carlsbad, California, USA). Line Human Coronary Artery Endothelial Cells (CAEC) (H1169) was from Cell Biologics (Chicago, Illinois, USA). Cytokine composition was assayed with the proteome Profiler mouse cytokine Array kit (ARY006, R&D Systems (Minneapolis, MN, USA).

### Animal studies

All the surgical procedures were performed in the Experimental Surgery Department of the Francisco de Vitoria University (Pozuelo de Alarcon, Spain). The procedures conformed to the Guide for the Care and Use of Laboratory Animals published by the US National Institutes of Health (NIH Publication No. 85–23, revised 1985), the Animal Welfare Ethics Committee, the EU Directive on experimental animals (63/2010 EU), and the related Spanish legislation (RD 53/2013). Male Young (8 weeks), Aged (24 months) ApoE $^{-/-}$  and Wild Type (C57BL/6J) mice were housed for 12 weeks on a high fat/cholesterol diet (21% butter fat and 0.21% cholesterol, Harlan TD 88137). Every 4 weeks, blood was drawn from each mouse at a maximum of 100  $\mu$ l/mouse. After 12 weeks of fat diet supplementation, animals were sacrificed, and aortas were isolated and collected for further processing.

### Human study

Human carotid endarterectomy specimens were obtained from 6 patients (3 men older than 80 and 3 men younger than 60) with >70% carotid stenosis, as demonstrated by digital subtraction angiography and Doppler ultrasonography. According to local ethics committee regulations, all samples were obtained as surgical residues (Scientific Committee, Ramon y Cajal University Hospital).

### Blood collection and plasma isolation

Animal blood samples were collected in sodium citrate (363086) (BD Vacutainer, Franklin Lakes, NJ, USA) from a submandibular (facial) bleed in mice. Blood samples were centrifuged at 400 g for 10 min, and the plasma was stored at  $-80^{\circ}\text{C}$ .

### Histology

On the day of the sacrifice of the animal, followed by exsanguination, the intact aorta was removed. The arterial wall was stained to identify the lipid Oil Red O (ORO). The aortas were immersed in formalin, washed thrice with PBS, and incubated for one hour in freshly prepared ORO (6 mg/mL in 60% isopropanol). Aortas were then washed for 30 min in 60% isopropanol. Under

a stereomicroscope, perivascular adipose tissue was gently removed with spring scissors (Castroviejo) and fine-tipped tweezers, cutting away the perivascular tissue while holding the vessel steady. Vessels were carefully transferred to a glass cover slide and photographed to determine cholesterol deposits, and lipid quantification was performed using image analysis software (Image J).

### Immunohistochemistry

Aortic sections were fixed in 4% formalin for 24 h, dehydrated through a graded ethanol series, and embedded in paraffin. Serial 4  $\mu$ m sections were deparaffinized, rehydrated, and subjected to immunostaining. After blocking with normal serum for 1 h at room temperature, sections were incubated overnight at 4 °C with the primary antibody (1:150). Following PBS washes, sections were incubated with a horseradish peroxidase-conjugated secondary antibody (1:500) for 1 h at room temperature. After additional PBS washes, signal detection was performed using the DAB system. Sections were visualized by brightfield microscopy, and images were analyzed using the ImageJ software.

### HAEC and CAEC cell culture

Primary cells HAEC and CAEC were grown in Endothelial Cell Medium (composed of 500 mL of basal medium (Cat. #1001), 25 mL of FBS (Cat. #0025), 5 mL of Endothelial Cell Growth Supplement (ECGS, Cat. #1052), and 5 mL of penicillin/streptomycin (P/S, Cat. #0503), all obtained from ScienCell Research Laboratories (Carlsbad, CA, USA)), and incubated 48 h in a humidified CO<sub>2</sub> incubator with 5% CO<sub>2</sub> at 37 °C. Following incubation, 2 mL of cell supernatant was collected and added to P1 endothelial cells for further evaluation of ES.

### Immunoblotting

Protein lysates were extracted from cell cultures with RIPA buffer to measure the levels of CAP1 and PCSK9. Proteins were separated by SDS-PAGE and transferred to PVDF membranes. The membranes were blocked with 3% BSA in 25 mM Tris, 150 mM NaCl, 0.05% Tween-20, pH 7.4 (T-TBS), washed, and incubated with the corresponding primary antibodies diluted 1:500 for one hour at room temperature. Subsequently, the membranes were washed 3 times with T-TBS and incubated with horseradish peroxidase-conjugated secondary antibodies 1:3000 for one hour for protein detection by chemiluminescence. GAPDH,  $\beta$ -Tubulin, and Ponceau Red (when blotting proteins from culture medium, 15 min staining followed by 2x washes with PBS) levels were used as loading controls.

### Isolation extracellular vehicles

Mouse plasma was centrifuged at 2400G for 15 min at 4 °C to remove dead cells and debris (Eppendorf Centrifuge 5415 R). Three additional rounds of centrifugation were then performed: (1) 2,400  $\times$  g for 15 min at 4 °C. (2) 12,500  $\times$  g for 5 min at 4 °C. (3) 20,500  $\times$  g for 50 min at 4 °C. After centrifugation, the pellets were resuspended in PBS (double filtered through 0.22  $\mu$ m filters) in a volume equal to the initial volume of supernatant and subjected to test centrifugations at 10,000G. Finally, the supernatant was collected, determined for further studies, and quantified by BCA.

EV validation in terms of size and concentration was conducted at the core facilities of "Hospital Universitario La Paz, Madrid, Spain", utilizing the NanoSight LM10 system (Malvern Panalytical, Worcestershire, United Kingdom). This system is widely used for nanoparticle tracking analysis (NTA), enabling precise measurements of size distributions and concentrations of EVs in liquid samples.

To assess ES, endothelial cells were seeded at 85% confluence and pre-treated once with 30  $\mu$ g isolated EVs from young and old ApoE<sup>-/-</sup> mice for 24 h in PBS. Subsequently, the medium was removed, and cells were collected for immunoblotting. To evaluate senescence in mice, two injections of 300  $\mu$ g EVs in PBS were administered twice a week after 12 weeks of a high-fat diet (HFD).

### SiRNA transfection

HAEC and CAEC were seeded in 6 multi-well plates with 2 ml of culture medium. Following the manufacturer's protocol, CAP1 siRNA transfection was performed using Opti-MEM Reduced Serum Medium, Lipofectamine RNAiMAX transfection reagent, and Human CAP1 Silencer Select siRNA. Transfection was performed for 24 h, and the transfecting medium was replaced with a complete growing medium. Cells were incubated for 24 h, then subjected to pCAP1 plasmid transfection and assayed for ES through the SA- $\beta$ -Gal Staining procedure, as detailed below.

### Plasmid transfection

HAEC and CAEC were seeded in 35 mm glass-bottom culture dishes and incubated for 24 h with Lipofectamine RNAiMAX transfection reagent (Thermo Fisher) containing 1  $\mu$ g/plasmid DNA (CAP1 (NM\_001105530)) (Origene) in medium supplemented with neomycin (500  $\mu$ g/ml). After the transfection reagents were removed, the cells were washed twice with a preheated culture medium and cultured for 48 h.

### SA- $\beta$ -gal staining

The senescence-associated  $\beta$ -galactosidase (SA- $\beta$ -Gal) was detected by fixing the cells with 1% formaldehyde, followed by PBS washing, and exposure to a solution containing X-Gal for 1 h at 37 °C. To assess HAEC and CAEC senescence in response to Evolocumab (Amgen S.A, Barcelona, Spain), cells were seeded and pre-treated with 100  $\mu$ g/ml Evolocumab. After a 24-hour incubation, the medium was removed, and the cells were washed with PBS. Subsequently, SA- $\beta$ -Gal staining was performed, as described above. For the in vivo  $\beta$ -galactosidase assay, 4  $\mu$ m paraffin-embedded aortic sections were fixed on microscopy slides for 10 min with 1% paraformaldehyde, followed by washing with PBS. Subsequently, the samples were incubated with the optimal X-gal concentration, following the manufacturer's protocol, for 1 h at 37°C.

### Proteomic studies

The proteomic analysis was performed at "Servicio de Central de Apoyo a la Investigacion, Universidad de Malaga (SCAI, Malaga, Spain). Protein concentration from EVs was assessed using the Pierce™ BCA assay, and samples were normalized to ~1  $\mu$ g/ $\mu$ L. Gel-assisted proteolysis was performed by entrapping proteins in a polyacrylamide gel matrix, followed by in-gel digestion with trypsin. Peptides were extracted using acetonitrile (ACN) and formic acid (FA), then dried and resuspended in 0.1% FA. Samples were analyzed using an Easy nLC 1200 UHPLC system coupled to a Q-Exactive HF-X Hybrid Quadrupole-Orbitrap mass spectrometer (Thermo Fisher Scientific, Waltham, MA, USA). Peptides were separated on a PepMap RSLC C18 analytical column, using a gradient of solvent A (0.1% FA in water) and solvent B (0.1% FA in 80% ACN). MS/MS spectra were acquired and processed in Proteome Discoverer™ 2.4 with SEQUEST® HT, EVs protein identification was performed against the *Mus musculus* UniProtKB database (version 2023-03-01). The Percolator algorithm was applied for validation, maintaining a strict false discovery rate (FDR) of <1%. Label-free quantification was performed using the Minora feature in Proteome Discoverer™ 2.2, normalizing precursor intensities based on total peptide amount. To ensure data quality, blank runs were performed before each injection, and a standard sample was included in each batch. The Benjamini-Hochberg correction was applied to control the false discovery rate (FDR) in multiple comparisons and to compute q-values, utilizing an R package to ensure statistical reliability and robustness. For protein classification, the FunRich software version 3.1.4 (available at <http://www.funrich.org>) was used, with a significance level set at 0.05. to perform enrichment analysis based on the Wikipathways and KEGG databases. A volcano plot was generated using the Life Sciences Mass Spectrometry Software (Thermo Fisher

Scientific, Waltham, MA, USA). The graph was created by plotting the log<sub>2</sub> fold change (FC) of the identified proteins against their corresponding adjusted -log<sub>10</sub> P-values. Proteins with an FC >1.3 were considered upregulated, while those with an FC <1.3 were classified as downregulated. A P-value of less than 0.05 was used as the threshold for statistical significance in all analyses.

### Cytokine array

We simultaneously detected a total of 36 mouse cytokines, chemokines, and acute-phase proteins from EVs ApoE-null mice using the Proteome Profiler Cytokine Array Kit ARY006 (R&D Systems, Minneapolis, MN, USA). This membrane-based antibody array enables the parallel assessment of relative levels of specific mouse cytokines and chemokines, following the manufacturer's instructions.

### Statistical analysis

All data were analyzed in a statistical software package (SPSS 22.0, SPSS Inc., Chicago, IL, USA). All values are given as a mean  $\pm$  SD. Significance is reported at the 5% level. Whenever comparisons were made with the common control, differences were tested by analysis of variance followed by Dunnett's modification of the t-test. The small sample size (N) made it challenging to determine normality, so we first assessed the normality of the data using the Shapiro-Wilk test. Given the violation of normality, we opted for a non-parametric alternative, the Mann-Whitney U test. Statistical significance was inferred for P values less than 0.05. In addition, to illustrate significant differences in protein expression between groups, a Volcano diagram was produced using the Life Sciences Mass Spectrometry Software (Thermo Fisher Scientific, Waltham, MA, USA).

## Results

### Aged mice lacking ApoE are more prone to developing atherosclerosis

To prove that atherosclerosis is an aging-related disorder, we fed young (8 weeks) and aged (24 months) ApoE null mice a regular high-fat/cholesterol diet at the same time, resulting in the development of more aortic lipid deposition and plaque lesions in older animals relative to their younger counterparts (Fig. 1AB). To assess whether the release of circulating EV in atherosclerosis may trigger an ES-associated programmed stress response, we first established a model of endothelial replicative senescence assay in HAEC and CAEC primary cell cultures spanning passages P1 through P12 and using b-Gal-staining and the expression of p16 as indicators. The rise in ES became notably pronounced at P5 for both cell types (Supplementary Fig. 1), underscoring the escalating manifestation of endothelial aging with consecutive cell passages.

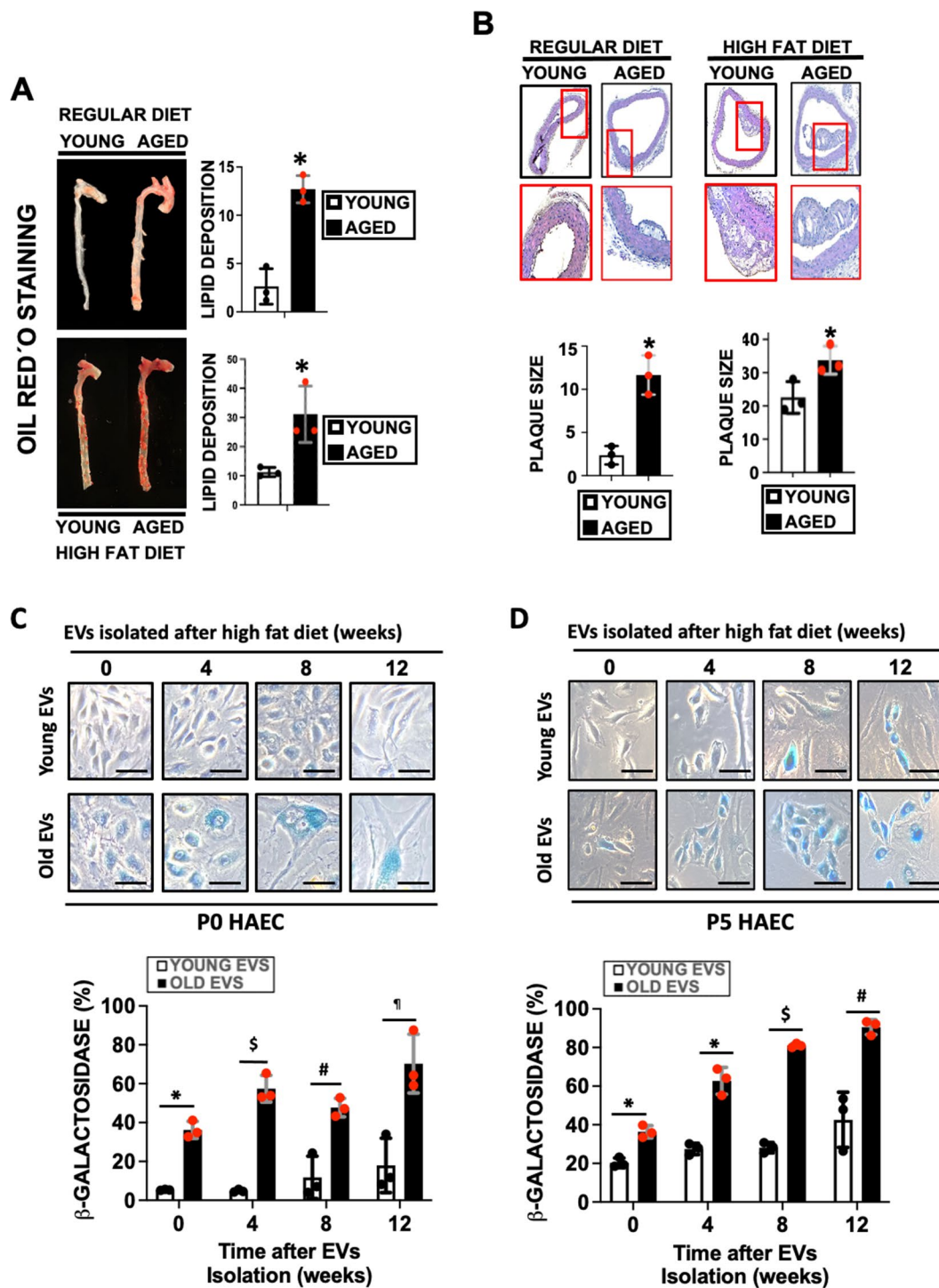


**Fig. 1** Atherosclerosis-induced ApoE KO mice were fed a high-fat diet. **A.** Representative images of Aortic Oil Red O staining from young and aged atherosclerotic ApoE null mice fed a regular or a high-fat diet for 8 weeks ( $N=3$  mice/group. Mean  $\pm$  ScD.  $*p < 0.05$  young vs. aged aortas). **B.** Representative Eosin/Hematoxylin staining of aortic sections of the same mice as in (A) ( $N=3$  Mean  $\pm$  SD.  $*p < 0.01$  Young vs. Aged). **C.** Representative  $\beta$ -galactosidase staining of P0 HAEC incubated with EVs from aged and young ApoE null mice and isolated at indicated times ( $N=3$  Mean  $\pm$  SD.  $*p < 0.01$ ,  $\#p < 0.01$ ,  $\$p < 0.001$ ,  $\uparrow p < 0.0001$  Young EVs vs. Aged EVs). **D.** Representative B-gal staining of P5 HAEC incubated with the same EVs as in (B) ( $N=3$  Mean  $\pm$  SD.  $*p < 0.001$ ,  $\#p < 0.0001$  Young EVs vs. Aged EVs). Scale bar = 50  $\mu$ m

To test whether atherosclerosis-induced senescence-associated secretory phenotype (SASP) may induce ES, we isolated blood-circulating EVs (identified by NTA analysis and a detailed cytokine-chemokine profile, Supplementary Fig. 2) from both young and aged ApoE-deficient mice fed with high-fat diet at four different time points (0, 4, 8, and 12 weeks after feeding, Supplementary Fig. 2A), and added to primary young endothelial cell cultures (passage P0), which do not exhibit signs of endothelial senescence (Supplementary Fig. 1). Remarkably, all EVs isolated from aged atherosclerotic mice induced endothelial senescence in P0 endothelial cell cultures (Fig. 1C). In contrast, when added to P5 ECs, EVs derived from young mice and collected at 4, 8, and 12 weeks experienced a significant delay in inducing a senescent phenotype (Fig. 1D). These findings underscore the distinct aging-related effects of atherosclerosis-inducing circulating EVs (of yet unknown origin) on endothelial cell senescence and offer new insights into the potential mechanisms driving age-related susceptibility to atherosclerosis. A detailed analysis of EV characterization by NTA, together with SASP-associated component composition, in which the level of 36 cytokines, chemokines, growth factors, and other SASP regulatory elements (see methods for details) was further assayed (Supplementary Figs. 2B–C).

#### **Circulating EVs from atherosclerotic mice exhibit a proteomic signature consistent with aging and lipid metabolism**

We conducted protein mass spectrometry in isolated blood circulating EVs from young and aged atherosclerotic ApoE null mice fed with the high-fat diet for 8 weeks using the Q Exactive™ HF-X Hybrid Quadrupole-Orbitrap mass spectrometer, identifying a total of 424 differentially expressed proteins. The identification of Intercellular Adhesion Molecule 1 (ICAM-1), von Willebrand Factor (vWF), and Vascular Endothelial Growth Factor Receptor 3 (VEGFR-3) among the identified proteins supports the notion that a subset of the EVs originates from endothelial cells. Further analysis through the STRING platform revealed 14 clusters of interacting proteins. Additionally, utilizing the FUNRINCH Functional Enrichment analysis tool [10], we comprehensively analyzed protein functionality, pinpointing significant interactions related to biological and molecular functions, including aging, lipid metabolism, and cell adhesion (Fig. 2AB). After thoroughly examining proteins showing distinct patterns between aged and young mice, four cargo proteins of interest were upregulated. A resulting Volcano Plot illustrated the differentially expressed proteins between the two groups (Fig. 2C). Particular emphasis is placed on Cyclase-associated protein 1 (CAP1), a cytoskeletal component that shows differential presence

in EVs from aged versus young atherosclerotic ApoE-null mice. Interestingly, CAP1 has been identified as a crucial partner of PCSK9 [9, 11], playing a significant role in the degradation of LDL receptors. While CAP1 was predominantly found in aged EVs, PCSK9 was present in young and aged EVs without a noticeable difference.

#### **CAP1 promotes ES in HAEC and CAEC**

To investigate the role of CAP1 in ES, we observed a significant increase in endogenous CAP1 expression over time in HAEC, CAEC (Fig. 3A), and culture media from passages 1–12 (Fig. 3B). Conditioned media collected from senescent endothelial cells at different passages 1–12 HAEC and CAEC were added to endothelial cell cultures at passage 1 HAEC and CAEC. In both cases, an increase in endothelial senescence was observed following incubation with this media. (Fig. 3C).

To determine the role of CAP1 in ES, we silenced CAP1 using specific small interfering RNA (CAP1-siRNA, see methods for details), which significantly reduced senescent activity in both cell types at passage 10 (P10), indicating that CAP1 promotes ES (Fig. 3D). To confirm the impact of CAP1 on ES, we conducted a validation study wherein we reinstated CAP1 in CAP1-silenced endothelial cells by transfecting pCAP1, a plasmid housing the CAP1 cDNA. Remarkably, pCAP1-induced exogenous CAP1 overexpression successfully reinstated the ES phenotype compromised in CAP1-silenced cells. (see methods for details) (Fig. 3E). To validate this finding, we isolated EVs from CAP1-silenced HAEC and CAEC and incubated them with P1 HAEC and CAEC. EVs from P5 HAEC and CAEC induced p16 expression in P1 endothelial cells. In contrast, CAP1-silenced EVs failed to induce p16, suggesting that CAP1 is required for EV-mediated senescence (Supplementary Fig. 3A).

Previous studies have demonstrated that CAP1 contributes to the nuclear translocation of the proinflammatory transcription factor NFκB in endothelial HUVECs [8]. To investigate the role of NFκB in CAP1-induced endothelial senescence (ES) in HAEC and CAEC, we treated P5 HAEC and CAEC with the NFκB activation inhibitor BAY11-7083 (10μM for 24 h). This treatment resulted in a significant reduction in the senescence marker p16. Notably, when NFκB inhibition was combined with CAP1 silencing, p16 expression was nearly undetectable (Supplementary Fig. 3B).

PCSK9 levels, on the other hand, remained constant in healthy and senescent HAEC and CAEC (Fig. 3F). To exclude the role of PCSK9 in CAP1-induced ES, we incubated ECs in the presence of 100 μg/ml PCSK9 inhibitor Evolocumab, finding no differences in ES in both cell types (Fig. 3G) and in overexpressing CAP1 (pCAP1) in CAP1-silenced cells (Fig. 3H; see methods for details),

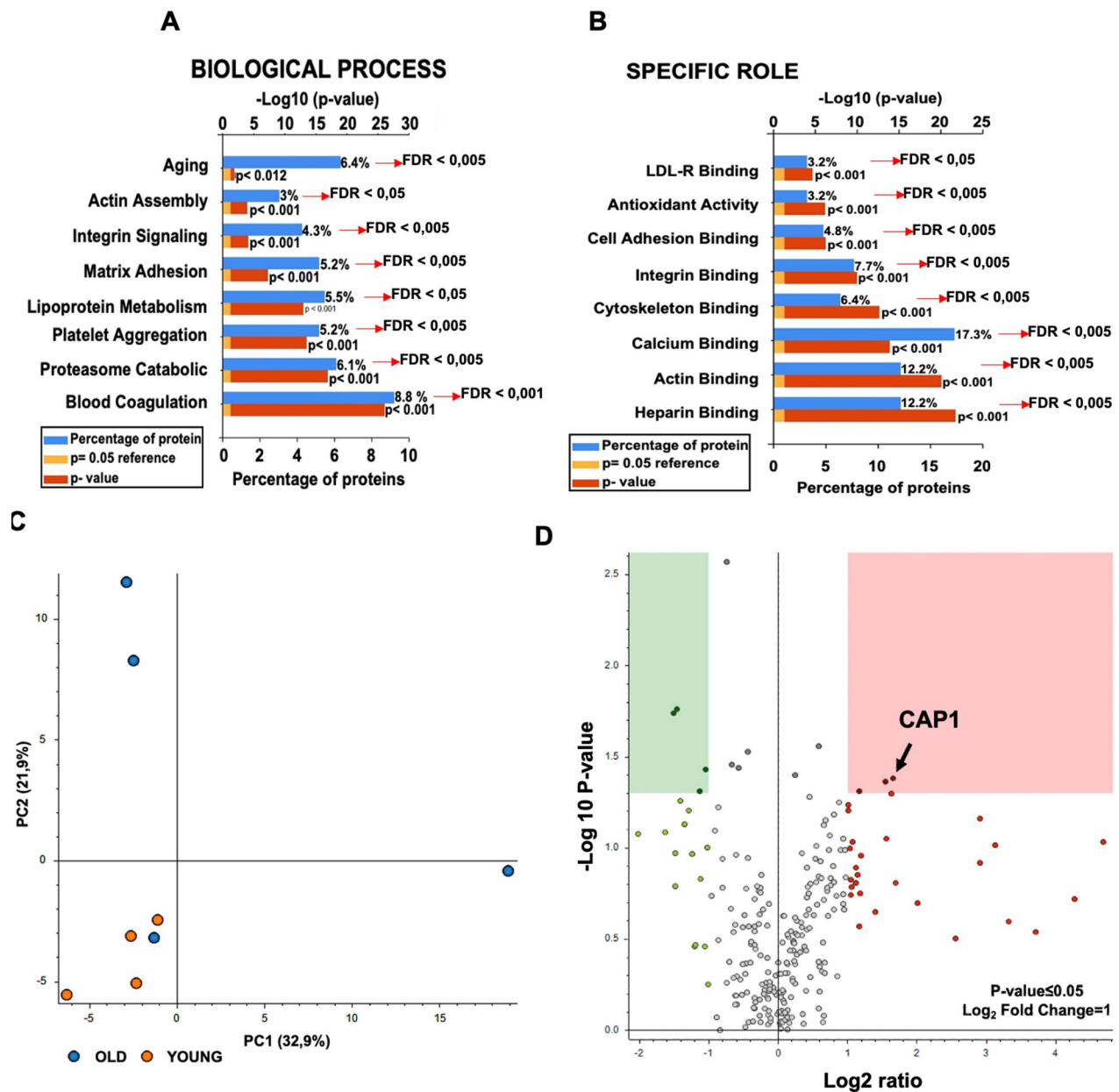


**Fig. 2** Proteomic analysis of EVs isolated from young and aged ApoE KO mice. **A, B.** Functional enrichment analysis of proteins present in blood circulating EVs from aged vs. young atherosclerotic ApoE null mice. **C.** Differences between young and aged EV samples, as well as the variability within each group, visualized through Principal Component Analysis (PCA). **D.** The volcano plot represents the quantitative proteomics data of samples, highlighting proteins with significant differential abundance. In this plot, proteins with statistical significance are defined as those with a  $-\log_{10}$  p-value  $> 1.3$  (y-axis). Statistically underexpressed proteins (green square) have a  $\log_2$  fold change  $\leq -1$ , while statistically overexpressed proteins (red square) have a  $\log_2$  fold change  $\geq +1$  (x-axis)

suggesting that CAP1-induced ES is independent of PCSK9.

CAP1 levels in other cell types, including vascular smooth muscle cells, macrophages, and fibroblasts, remained unchanged in response to cell passaging (Supplementary Fig. 3C).

**CAP1 exhibits differential expression in mouse aortas and human carotid endarterectomies from young versus aged individuals**

Our observations revealed a significant upregulation of CAP1 in aortic sections from aged atherosclerotic mice compared to their younger counterparts (Fig. 4A). Additionally, CAP1 levels were analyzed in human endarterectomy samples, revealing that older patients ( $> 80$  years) exhibited higher levels of CAP1 compared to younger

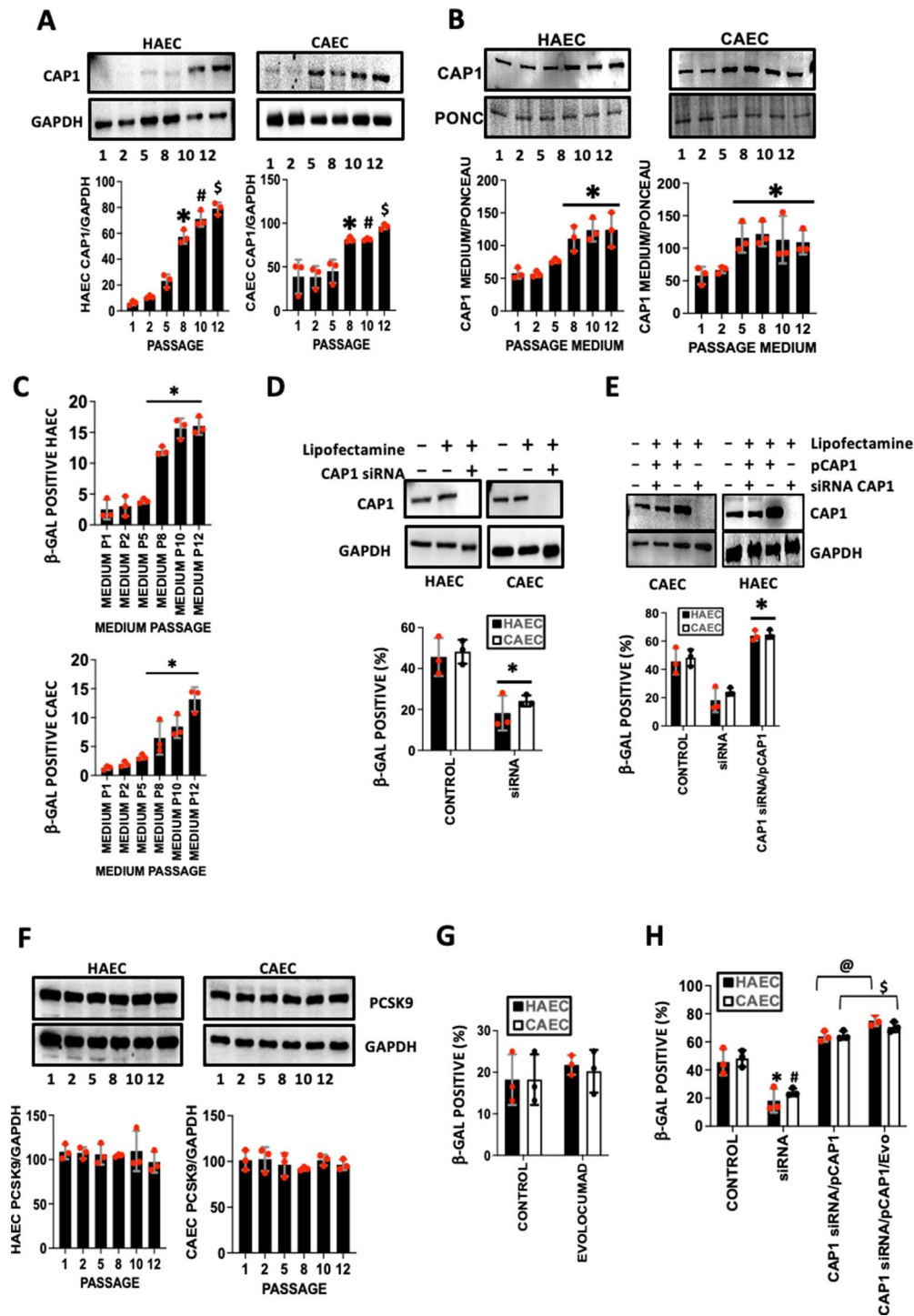


**Fig. 3** CAP1 induces ES in HAEC and CAEC. **(A)** Representative immunoblot detection of CAP1 in HAEC and CAEC from P1 to P12. ( $N=3$  Mean  $\pm$  SD.  $*p < 0.05$ .  $\#p < 0.01$ .  $\$p < 0.001$  P1 vs. selected passages). **(B)** Representative immunoblot detection of CAP1 in conditioned medium of HAEC and CAEC from P1 to P12. ( $N=3$  Mean  $\pm$  SD.  $*p < 0.05$ . P1 vs. selected passages). **(C)** Senescence-associated B-gal (SABG) staining of P1 HAEC and CAEC incubated 24 h with 2 ml culture medium from P1-12 HAEC and CAEC as indicated ( $N=3$  Mean  $\pm$  SD.  $*p < 0.05$ .  $**p < 0.01$ . P1 vs. selected passages). **(D)** CAP1 silenced HAEC and CAEC representative immunoblot shows.  $N=3$  Mean  $\pm$  SD.  $*p < 0.05$  CAP1 siRNA vs. CONTROL. **(E)** CAP1 silenced HAEC and CAEC overexpressing CAP1 (after transfection of pCAP1), as shown by representative immunoblot.  $N=3$  Mean  $\pm$  SD.  $*p < 0.05$  CAP1 siRNA vs. CAP1 siRNA/pCAP1. **(F)** Representative immunoblot detection of PCSK9 in HAEC and CAEC from P1 to P12. ( $N=3$  Mean  $\pm$  SD). **(G)** ES assay in HAEC and CAEC incubated with 100 mM PCSK9 inhibitor Evolocumab.  $N=3$  Mean  $\pm$  SD. **(H)** ES assay in Evolocumab incubated cells as in B.  $N=3$  Mean  $\pm$  SD,  $*p < 0.05$ , and  $\#p < 0.05$  CONTROL vs. CAP1 siRNA in HAEC and CAEC, respectively.  $@p < 0.05$  HAEC CAP1 siRNA/pCAP1 and CAP1 siRNA/pCAP1/Evo vs. CONTROL.  $\$p < 0.05$  CAEC CAP1 siRNA/pCAP1 and CAP1 siRNA/pCAP1/Evo vs. CONTROL.

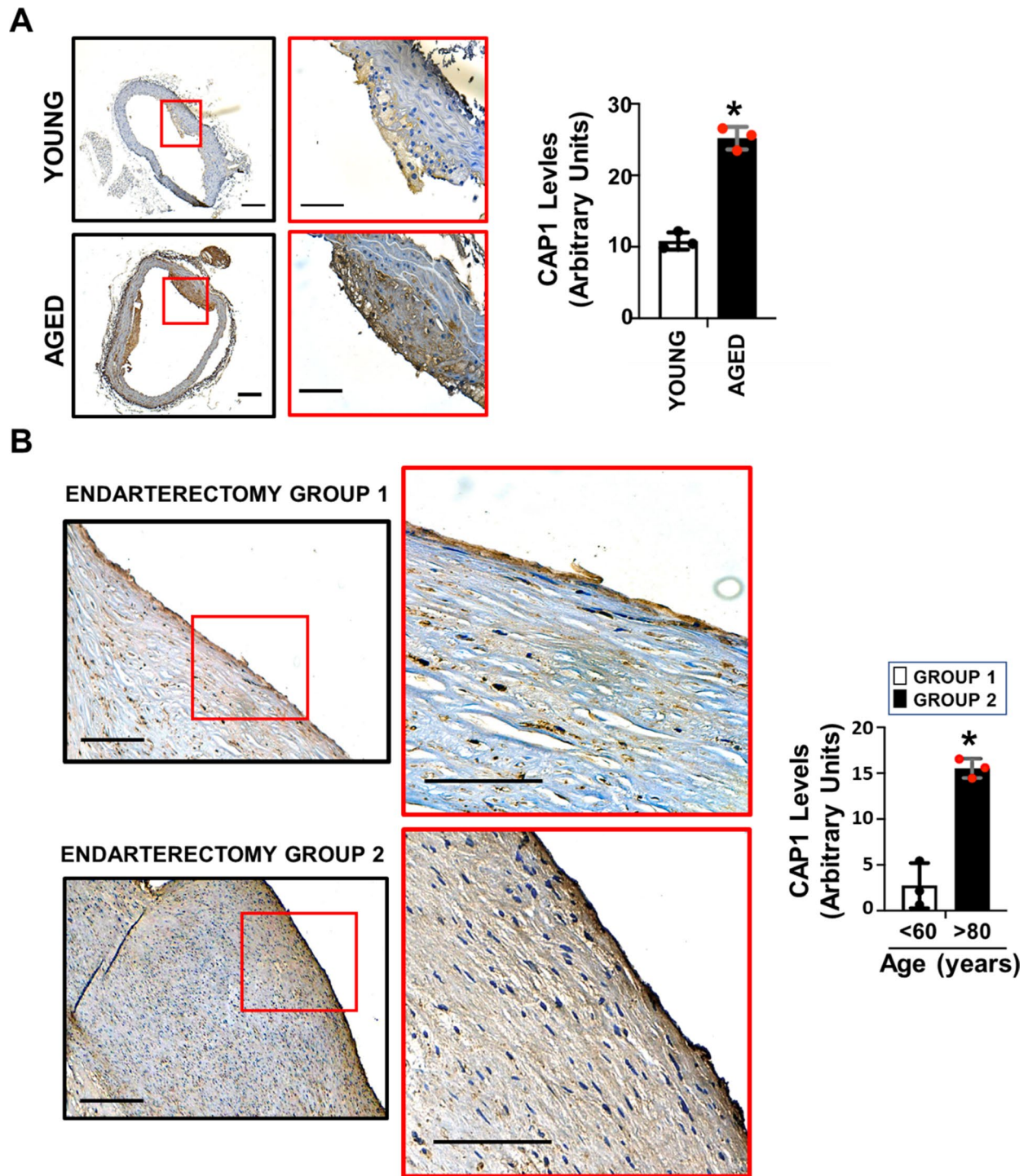


**Fig. 4** Expression of CAP1 in mouse and human atherosclerosis. **(A)** Representative immunohistochemistry detection of CAP1 in aortic plaques from young and aged ApoE atherosclerotic mice. Scale bars 50  $\mu$ m.  $N=3$  mice/group.  $*p < 0.05$  Young vs. Aged ApoE KO mice. **(B)** Representative immunohistochemistry detection of CAP1 in human carotid endarterectomy sections from group 1 (patients younger than 60 years, upper panels) and group 2 (patients older than 80 years, lower panels). Scale bars 100  $\mu$ m.  $N=3$  patients/group.  $P < 0.005$  group1 vs. group2

patients (<60 years) (Fig. 4B). However, to more precisely evaluate the role of CAP1 in humans, a substantial increase in sample size will be necessary.

### CAP1 containing EVs from aged ApoE KO mice increase ES in WT mice and elicit an atheroma phenotype in response to a high-fat diet

To investigate the role of CAP1 in ES in vivo, we isolated EVs from ApoE knockout animals and observed a significant increase in CAP1 levels in EVs from aged mice (Fig. 5A), which are the same mice exhibiting more significant aortic lipid accumulation (Fig. 1A). Following confirmation that CAP-1-containing EVs trigger ES in endothelial cell cultures (Fig. 1CD), we investigated whether EVs may also influence ES in vivo.

We IV injected 300  $\mu\text{g}/\text{week}$  EVs isolated from young (Fig. 5BD) and aged ApoE KO mice (Fig. 5CE) into WT mice fed with regular (Fig. 5BC) and high-fat diet

(Fig. 5DE). Two weeks after injection, a pronounced increase in  $\beta$ -gal-positive staining was observed in aortic rings from WT mice injected with aged EVs, regardless of diet consumed (Fig. 5CE vs. 5BD). Additionally, a p16 immunohistochemical detection in the same sections further confirmed the senescence phenotype (Supplementary Fig. 4). HE staining of aortic sections from WT mice yielded an unexpected phenotype consisting in intraluminal atheroma-like structures when fed with high-fat diet (Fig. 5E), in comparison with the aortic sections from mice fed with regular diet (Fig. 5D). Overall, our findings suggest that CAP1-containing EVs isolated from aged atherosclerotic mice (Fig. 5A), induce endothelial senescence and promote the progression of an atherosclerotic phenotype in WT mice on a high-fat diet.

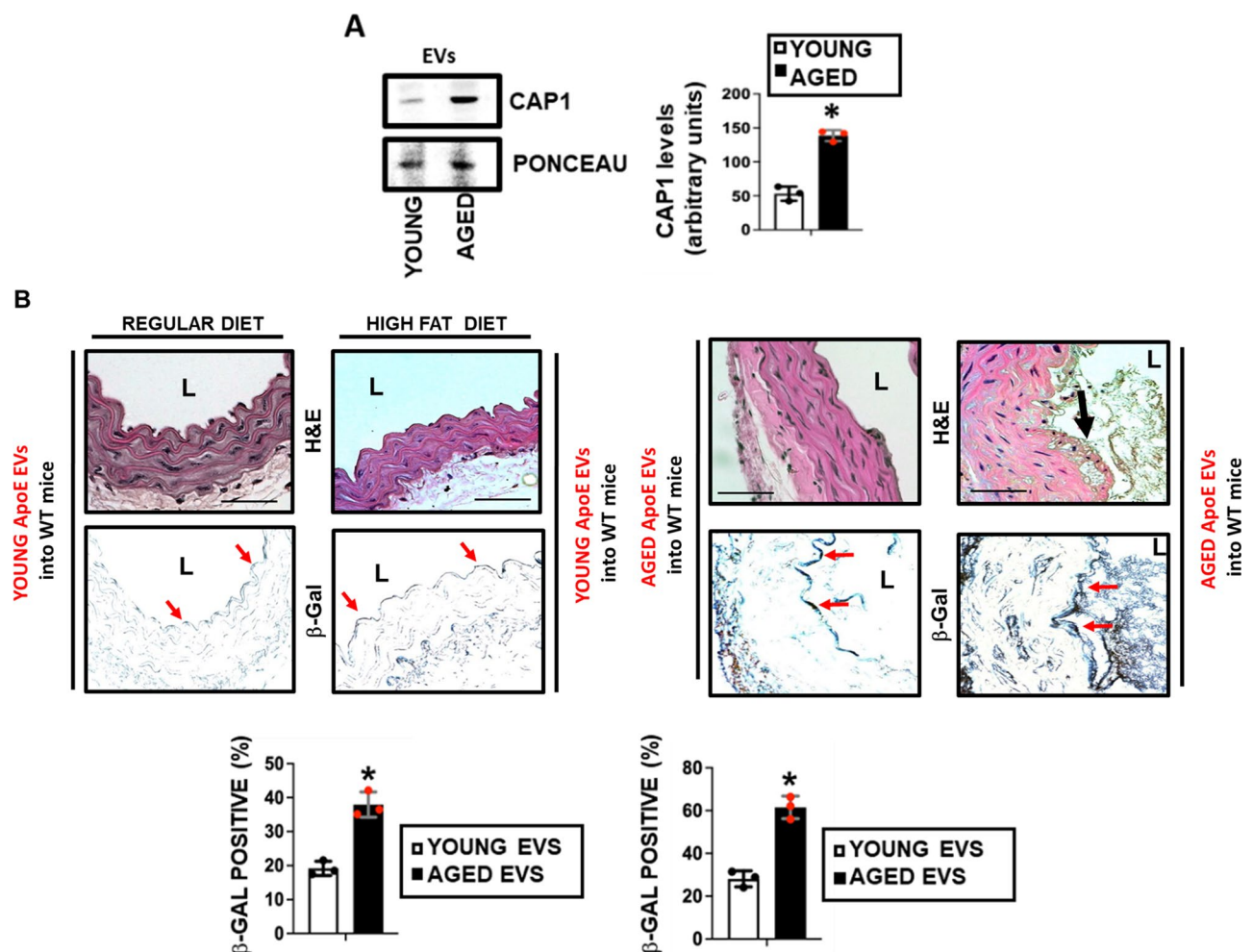


**Fig. 5** EVs from aged ApoE knockout mice induce ES in WT animals. **A**. Representative immunoblot detection of CAP1 from blood circulating EVs isolated from young and aged ApoE knockout mice ( $N=3$  Mean  $\pm$  SD. \* $p < 0.05$  Young vs. Aged ApoE EVs). **B-E**. Hematoxylin/Eosin (H&E) staining (upper panels) and b-Galactosidase (b-Gal) assay (lower panels) in aortic sections of WT mice fed with regular diet (**B, C**) or high-fat diet (**D, E**), and injected with EVs from young (**B, D**), or aged (**C, E**) ApoE KO mice as indicated. Scale bars 100  $\mu\text{m}$  ( $N=3/\text{group}$ )

### Injection of CAP1-containing EVs isolated from aged ApoE KO mice increases atherosclerosis in young ApoE KO mice

The above data led us to explore whether CAP1-containing EVs could lead to ES and atherosclerosis in young ApoE KO mice. We confirmed that younger animals injected with EVs from aged ApoE-null mice developed atheroma plaques similar to those found in older specimens, displaying extensive necrotic cores, together with increased  $\beta$ -Gal-positive aortic staining (Fig. 6 right panels) and intraplaque calcium deposits, as shown by Von Kossa staining of the same aortic sections, compared to the aortas from mice injected with EVs from young animals. Conversely, when administering EVs derived from young ApoE null mice, we observed reduced senescence and smaller plaque formation (Fig. 6 left panels). Collectively, our data highlight CAP1-containing EVs as a new molecular target against senescence and atherosclerosis in mice.

### Discussion

The current study identifies cyclase-associated protein 1 (CAP1) as a novel potential marker of aging-related ES in atherosclerosis. Aging-related atherosclerosis became evident when aged and young ApoE-null mice were concurrently fed a high-fat diet, revealing increased aortic lipid deposition and atheroma plaque formation in aged mice, along with a distinct EV composition. The role of circulating EVs in ES was confirmed through a replicative senescence assay in HAEC and CAEC, where EVs from aged ApoE KO mice induced ES in healthy cells. A proteomic analysis further identified CAP1 as a key cargo component predominantly enriched in EVs from aged mice.

Aging is a leading cause of endothelial dysfunction, an essential hallmark for the onset and progression of cardiovascular complications, including atherosclerosis [12]. In this regard, endothelial senescence (ES) is an age-related complication that contributes to the progression of atherosclerosis over time [13]. However, the factors triggering ES remain poorly understood [14, 15], highlighting the need for further investigation to better elucidate these mechanisms. Here, we found that CAP1 could represent a novel target for preventing ES, and ES-associated atherosclerosis.

CAP1 is an actin disassembly protein involved in actin dynamics [16]. Recently, the dysregulation of CAP1 has drawn attention to its association with several diseases, particularly emphasizing its role in developing metabolic, renal, and cardiovascular diseases [17–19]. Several lines of evidence have highlighted the implication of CAP1 in atheroma plaque development, and recent findings suggest a molecular mechanism by which CAP1 influences PCSK9-mediated inhibition of LDL receptor (LDL-r)

recycling. Here, we identify a new role for CAP1 in atherosclerosis progression.

We have identified CAP1 as a cargo component predominantly present in EVs derived from ApoE null mice. The implication of CAP1 in ES became evident in CAP1-silenced HAEC and CAEC, in which ES was significantly reduced, while restoration of CAP1 cDNA into CAP1-silenced endothelial was enough to rescue the ES phenotype. Notably, atherosclerotic lesions in young mice injected with EVs from aged animals resembled those currently present in older animals, with thickened necrotic cores, calcium deposition, and heightened senescence, suggesting CAP1 as a novel candidate for targeting ES associated with the progression of atherosclerosis.

Given the relationship between CAP1 and PCSK9 in atherosclerosis [9], we hypothesized that PCSK9 might also contribute to CAP1-induced ES, as evidenced by the requirement of CAP1 in PCSK9-mediated inhibition of LDLr recycling [19]. In line with this observation, it's worth noting that PCSK9 is expressed in vascular endothelial cells, and as with CAP1, the levels of PCSK9 also increase in aged HAEC [20]. However, our data suggest a CAP1-independent effect of PCSK9 on ES, consistent with recent findings identifying its role as a novel diagnostic biomarker in acute myocardial infarction AMI [21]. Interestingly, this study revealed that CAP1 expression increased in the supernatants of ox-LDL-induced HUVECs in a dose- and time-dependent manner. Additionally, CAP1 inhibited cell proliferation, promoted inflammation, and activated NF- $\kappa$ B [8], a key transcription factor implicated in cellular senescence, as evidenced in this work, in which NF $\kappa$ B activation inhibition further reduced ES in CAP1-silenced cells.

Extracellular vesicles (EVs) are small bilayer nanoparticles released by nearly all cell types and secreted to many fluids, including plasma, serum, blood, urine, or spinal fluid. EVs are secreted in response to many pathological conditions, containing several cargo components [22], which may play a significant role in the progression of aging-related diseases, like Alzheimer's disease [23], chronic kidney disease [24], and atherosclerosis [25]. Indeed, EVs from aged/injured tissues can propagate cellular senescence signals, as we found in atherosclerotic ApoE knockout mice. Indeed, the role of EVs in plaque development and maturation has been extensively investigated. ICAM-1 and PECAM-1 from EVs are transferred to endothelial cells, promoting adhesion and recruitment of monocytes [26] and neutrophils [27], and in many cases, EVs also elicit an inflammatory response through activation of NF- $\kappa$ B inflammatory transcription factor in ECs [28]. Whether EVs bind to ECs and transfer CAP1 along with other cargo components cannot be ruled out and remains subject to further investigation. Indeed,

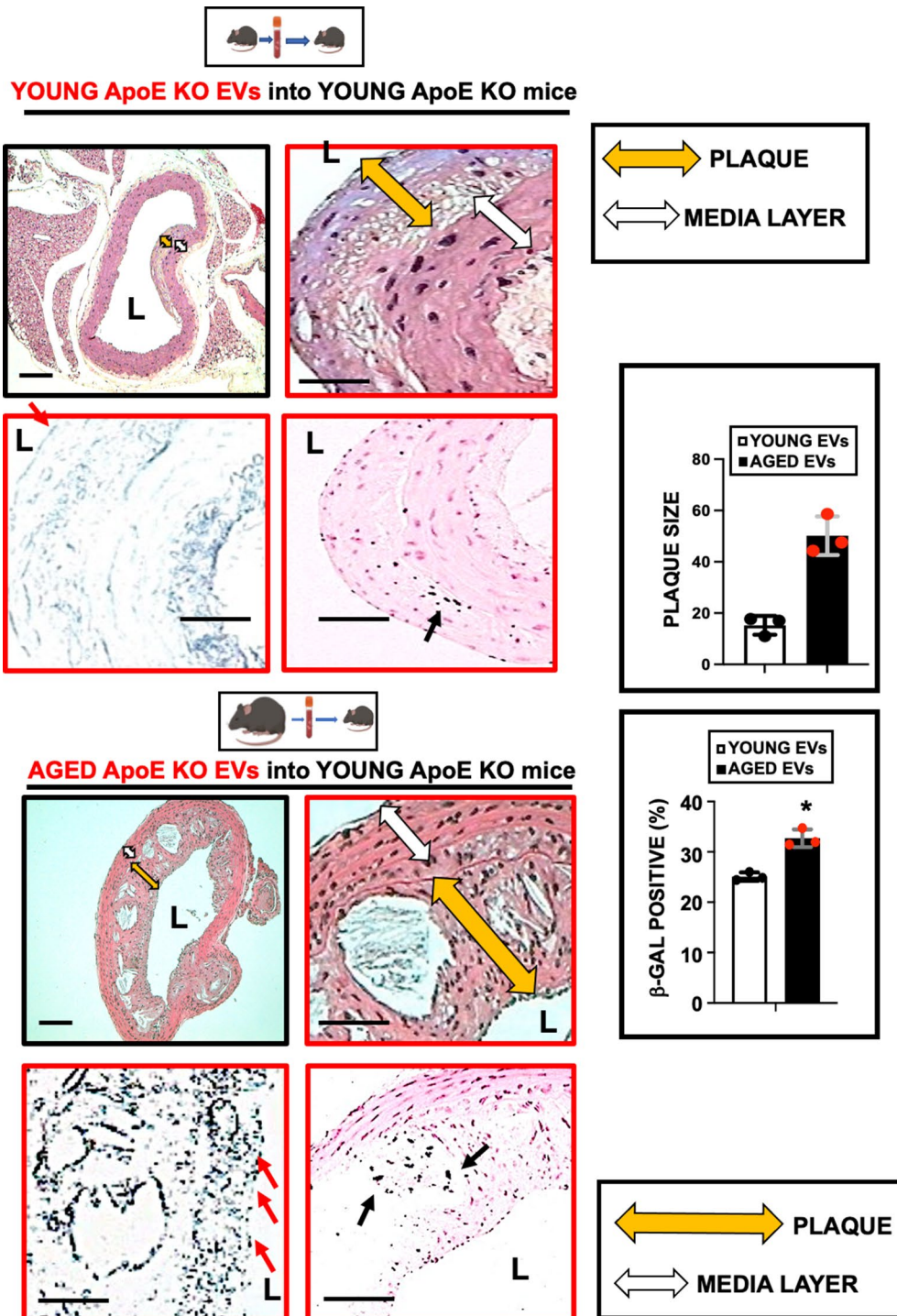


**Fig. 6** EVs from aged ApoE knockout mice induce ES and extensive atheroma plaque formation in young ApoE null mice. Hematoxylin/Eosin (H&E) staining (upper), β-Gal assay (lower left), and Von Kossa staining (lower right) in aortic sections of young ApoE knockout mice injected with EVs from young (upper panels) or aged (lower panels) ApoE KO mice. (Mean ± SD.  $N=3/\text{group}$  \* $p < 0.05$  EVs from aged vs. EVs from young ApoE KO mice). Orange arrows show atheromatous plaque thickness. White arrows indicate arterial medial thickness. Black arrows show intraplaque calcium deposits

ICAM-1 and other specific EC components including vWF, were differentially expressed in EVs from aged ApoE null mice.

Consistent with the above, several cargo components, from nucleic acids [29], metabolites [30], and proteins, have been reported so far, which may help to understand the progression of many complications. Multi-omics approaches have enabled the establishment of specific cargo elements of EVs in atherosclerosis [25], such as the release of adhesion molecules to endothelial cells, thereby promoting monocyte recruitment and adhesion [26] or specific microRNAs to atheroprone endothelium [31]. By using a proteomic approach, we identified novel EV components that could serve as potential molecular targets for senescence beyond chronological aging, in which CAP1 has emerged as a promising candidate linked to ES-related atherosclerosis. However, additional cargo elements beyond CAP1, such as non-coding RNAs, lipids, and proteins yet to be identified, may also play a significant role. Besides, whether CAP1 is solely responsible or it binds to other partners also requires further investigation. In this context, it is noteworthy that CAP1 is a receptor for the human resistin protein, participating in monocyte-mediated inflammation [32]. This interaction has implications for conditions such as coronary artery disease (CAD) [33] and atherosclerosis [34]. Furthermore, recent research has linked resistin secretion by alveolar macrophages to endothelial dysfunction [35].

Our study is the first to identify CAP1 as a novel molecular target in ES-associated atherosclerosis. However, certain limitations must be addressed, including the need for a larger in vivo sample size to ensure robust conclusions for future clinical applications. While we have identified specific endothelial cell markers and described a clear impact on ES progression and atheroma formation, further studies are required to comprehensively characterize all EV sources and clarify the molecular mechanisms governing EV uptake. For extended validation and potential clinical implementation, blood circulating CAP1 should be assessed.

### Supplementary Information

The online version contains supplementary material available at <https://doi.org/10.1186/s13062-025-00646-7>.

Supplementary Material 1

### Acknowledgements

We would like to acknowledge Marta Cano-Alonso for her valuable support.

### Author contributions

C.Z conceived and designed of the work. IH, LB, JD, LT, C.G-C, B.J-G and N.A performed experiments. J.L.Z and M.S analyzed data. C.Z and I.H interpreted figures and drafted manuscript. C.Z edited and revised manuscript and approved final version of manuscript. All authors viewed the paper and approved the version of the manuscript.

### Data availability

No datasets were generated or analysed during the current study.

### Declarations

#### Ethical approval and consent to participate

All the surgical procedures were performed in the Experimental Surgery Department of the Francisco de Vitoria University (Pozuelo de Alarcón, Spain). The procedures conformed to the Guide for the Care and Use of Laboratory Animals published by the US National Institutes of Health (NIH Publication No. 85–23, revised 1985), the Animal Welfare Ethics Committee, the EU Directive on experimental animals (63/2010 EU), and the related Spanish legislation (RD 53/2013).

#### Grants

This work was supported by research grants from (MS) Junta de Castilla La Mancha SBPLY/19/180501/000055; Co-financed by the European Union regional fund “a way to achieve Europe” and Instituto de Salud Carlos III; ISCIII PI20-00930 Co-financed by the European Union regional fund “a way to achieve Europe”; (CZ) Proyectos de i + D + I, from the program Investigación orientada a los retos de la sociedad, cofounded by Fondo Europeo de Desarrollo Regional (FEDER) A way to achieve Europe (MINECO/AEI/FEDER/EU SAF2017-87342-R), (MICINN/AEI/FEDER/EU PID2020-118371RB-I00), and “Proyectos de i + D + I, from the program Investigación orientada a los retos de la sociedad, cofounded by Fondo Europeo de Desarrollo Regional (FEDER) A way to achieve Europe PRUEBA DE CONCEPTO (MICINN/AEI/FEDER/EU PDC2021-121817-100) UFV research grant 2019.

#### Competing interests

The authors declare no competing interests.

Received: 22 January 2025 / Accepted: 29 March 2025

Published online: 06 April 2025

### References

1. Jia G, Arora AR, Jia C, Sowers JR. Endothelial cell senescence in aging-related vascular dysfunction. *Biochim Biophys Acta Mol Basis Dis*. Jul 1;1865(7):1802–1809, 2019. <https://doi.org/10.1016/j.bbadis.2018.08.008>
2. Han Y, Kim SY. Endothelial senescence in vascular diseases: current Understanding and future opportunities in senotherapeutics. *Exp Mol Med Jan*. 2023;55(1):1–12. <https://doi.org/10.1038/s12276-022-00906-w>.
3. Birch J, Gil J. Senescence and the SASP: many therapeutic avenues. *Genes Dev*. Dec 1;34(23–24):1565–1576, 2020 doi: <https://doi.org/10.1101/gad.343129.120>
4. Huang W, Hickson LJ, Eirin A, Kirkland JL, Lerman LO. Cellular senescence: the good, the bad and the unknown. *Nat Rev Nephrol Oct*. 2022;18(10):611–27. <https://doi.org/10.1038/s41581-022-00601-z>.
5. Takei Y, Yamada M, Saito K, Kameyama Y, Aihara T, Iwasaki Y, Murakami T, Kaiho Y, Ohkoshi A, Konno D, Shiga T, Takahashi K, Ikumi S, Toyama H, Ejima Y, Yamauchi M. Endothelium-Derived extracellular vesicles expressing intercellular adhesion molecules reflect endothelial permeability and sepsis severity. *Anesth Analg*. 2024;139(2):385–96. <https://doi.org/10.1213/ANE.0000000000006988>.
6. Abbas M, Jesel L, Auger C, Amoura L, Messas N, Manin G, Rumig C, León-González AJ, Ribeiro TP, Silva GC, Abou-Merhi R, Hamade E, Hecker M, Georg Y, Chakfe N, Ohlmann P, Schini-Kerth VB, Toti F, Morel O. Endothelial microparticles from acute coronary syndrome patients induce premature coronary artery endothelial cell aging and thrombogenicity: role of the Ang II/AT1 receptor/nadph Oxidase-Mediated activation of MAPKs and PI3-Kinase pathways. *Circulation Jan*. 2017;17(3):280–96. <https://doi.org/10.1161/CIRCULATIONAHA.116.017513>.
7. Mas-Bargues C, Borrás C, Alique M. The contribution of extracellular vesicles from senescent endothelial and vascular smooth muscle cells to vascular calcification. *Front Cardiovasc Med Apr*. 2022;15:9:854726. <https://doi.org/10.3389/fcvm.2022.854726>.
8. Jin D, Li X, Cong H, You B, Ma Y, Hu Y, Zhang J. Role of serum CAP1 protein in the diagnosis of patients with first-time acute myocardial infarction. *Med (Baltim)*. 2023;102(39):e34700. <https://doi.org/10.1097/MD.0000000000003470.0>.

9. Jang HD, Lee SE, Yang J, Lee HC, Shin D, Lee H, Lee J, Jin S, Kim S, Lee SJ, You J, Park HW, Nam KY, Lee SH, Park SW, Kim JS, Kim SY, Kwon YW, Kwak SH, Yang HM, Kim HS. Cyclase-associated protein 1 is a binding partner of proprotein convertase subtilisin/kexin type-9 and is required for the degradation of low-density lipoprotein receptors by proprotein convertase subtilisin/kexin type-9. *Eur Heart J Jan.* 2020;7(2):239–52. <https://doi.org/10.1093/eurheartj/ehz566>.
10. Pathan M, Keerthikumar S, Ang CS, Gangoda L, Quek CY, Williamson NA, Mouradov D, Sieber OM, Simpson RJ, Salim A, Bacic A, Hill AF, Stroud DA, Ryan MT, Agbinya JI, Mariadason JM, Burgess AW, Mathivanan S. FunRich: an open access standalone functional enrichment and interaction network analysis tool. *Proteom Aug.* 2015;15(15):2597–601. <https://doi.org/10.1002/pmic.2014.00515>.
11. Bertling E, Hotulainen P, Mattila PK, Matilainen T, Salminen M, Lappalainen P. Cyclase associated protein 1 (CAP1) promotes cofilin-induced actin dynamics in mammalian nonmuscle cells. *Mol Biol Cell May.* 2004;15(5):2324–34. <https://doi.org/10.1091/mbc.e04-01-0048>.
12. Tyrrell DJ, Goldstein DR. Ageing and atherosclerosis: vascular intrinsic and extrinsic factors and potential role of IL-6. *Nat Rev Cardiol Jan.* 2021;18(1):58–68. <https://doi.org/10.1038/s41569-020-0431-7>.
13. Minamino T, Miyauchi H, Yoshida T, Ishida Y, Yoshida H, Komuro I. Endothelial cell senescence in human atherosclerosis: role of telomere in endothelial dysfunction. *Circulation.* Apr 2;105(13):1541–4, 2002. <https://doi.org/10.1161/01.cir.0000013836.85741.17>
14. Diaz-Del Cerro E, Martinez de Toda I, Félix J, Baca A, De la Fuente M. Components of the Glutathione Cycle as Markers of Biological Age: An Approach to Clinical Application in Aging. *Antioxidants (Basel).* Jul 30;12(8):1529, 2023. <https://doi.org/10.3390/antiox12081529>
15. Huber J, Vales A, Mitulovic G, Blumer M, Schmid R, Witztum JL, Binder BR, Leitinger N. Oxidized membrane vesicles and blebs from apoptotic cells contain biologically active oxidized phospholipids that induce monocyte-endothelial interactions. *Arterioscler Thromb Vasc Biol. Jan;* 2002;22(1):101–7. <https://doi.org/10.1161/hq0102.101525>.
16. Jin ZL, Jo YJ, Namgoong S, Kim NH. CAP1-mediated actin cycling via ADF/cofilin proteins is essential for asymmetric division in mouse oocytes. *J Cell Sci.* Dec 5;131(23):jcs222356, 2018. <https://doi.org/10.1242/jcs.222356>
17. Zhang X, Pizzoni A, Hong K, Naim N, Qi C, Korkhov V, Altschuler DL. CAP1 binds and activates adenylate cyclase in mammalian cells. *Proc Natl Acad Sci U S A Jun.* 2021;118(24):e2024576118. <https://doi.org/10.1073/pnas.2024576118>.
18. Munjas J, Sopić M, Bogavac-Stanojević N, Kravljaca M, Miljković M, Simić-Ogrizović S, Spasojević-Kalimanovska V, Jelić-Ivanović Z. Serum resistin, adenylate cyclase-associated protein 1 gene expression, and carotid Intima-Media thickness in patients with End-Stage renal disease and healthy controls. *Cardiorenal Med.* 2020;10(1):51–60. <https://doi.org/10.1159/000503416>.
19. Fruchart Gaillard C, Ouadda ABD, Ciccone L, Girard E, Mikaëli S, Evagelidis A, Le Dévéhat M, Susan-Resiga D, Lajeunesse EC, Nozach H, Ramos OHP, Thureau A, Legrand P, Prat A, Dive V, Seidah NG. Molecular interactions of PCSK9 with an inhibitory nanobody, CAP1 and HLA-C: functional regulation of LDLR levels. *Mol Metab Jan.* 2023;67:101662. <https://doi.org/10.1016/j.molmet.2022.101662>.
20. Liu S, Wu J, Stolarz A, Zhang H, Boerma M, Byrum SD, Rusch NJ, Ding Z. PCSK9 attenuates efferocytosis in endothelial cells and promotes vascular aging. *Theranostics.* May 11;13(9):2914–2929, 2023. <https://doi.org/10.1016/j.theranu.2023.05.011>
21. Jin D, Li X, Cong H, You B, Ma Y, Hu Y, Zhang J. Role of serum CAP1 protein in the diagnosis of patients with first-time acute myocardial infarction. *Med Sept.* 2023;102(39):e34700. <https://doi.org/10.1097/MD.00000000000034700>.
22. van Niel G, D'Angelo G, Raposo G. Shedding light on the cell biology of extracellular vesicles. *Nat Rev Mol Cell Biol Apr.* 2018;19(4):213–28. <https://doi.org/10.1038/nrm.2017.125>.
23. Ruan Z, Pathak D, Venkatesan Kalavai S, Yoshii-Kitahara A, Muraoka S, Bhatt N, Takamatsu-Yukawa K, Hu J, Wang Y, Hersh S, Ericsson M, Gorantla S, Gendelman HE, Kaye R, Ikezu S, Luebke JI, Ikezu T. Alzheimer's disease brain-derived extracellular vesicles spread tau pathology in interneurons. *Brain.* Feb 12;144(1):288–309, 2021. <https://doi.org/10.1093/brain/awaa376>
24. Yin S, Zhou Z, Fu P, Jin C, Wu P, Ji C, Shan Y, Shi L, Xu M, Qian H. Roles of extracellular vesicles in ageing-related chronic kidney disease: demon or Angel. *Pharmacol Res Jul.* 2023;193:106795. <https://doi.org/10.1016/j.phrs.2023.106795>.
25. Blaser MC, Buffolo F, Halu A, Turner ME, Schlotter F, Higashi H, Pantano L, Clift CL, Saddic LA, Atkins SK, Rogers MA, Pham T, Vromman A, Shvartz E, Sukhova GK, Monticone S, Camussi G, Robson SC, Body SC, Muehlschlegel JD, Singh SA, Aikawa M, Aikawa E. Multiomics of Tissue Extracellular Vesicles Identifies Unique Modulators of Atherosclerosis and Calcific Aortic Valve Stenosis. *Circulation.* Aug 22;148(8):661–678, 2023. <https://doi.org/10.1161/CIRCULATIONAHA.122.063402>
26. Rautou PE, Leroyer AS, Ramkhalawon B, Devue C, Duflaut D, Vion AC, Nalbonte G, Castier Y, Leseche G, Lehoux S, Tedgui A, Boulanger CM. Microparticles from human atherosclerotic plaques promote endothelial ICAM-1-dependent monocyte adhesion and transendothelial migration. *Circ Res.* Feb 4;108(3):335–43, 2011. <https://doi.org/10.1161/CIRCRESAHA.110.237420>
27. Kuravi SJ, Harrison P, Rainger GE, Nash GB. Ability of Platelet-Derived Extracellular Vesicles to Promote Neutrophil-Endothelial Cell Interactions. *Inflammation.* 2019;42(1):290–305. <https://doi.org/10.1007/s10753-018-0893-5>.
28. Tang N, Sun B, Gupta A, Rempel H, Pulliam L. Monocyte exosomes induce adhesion molecules and cytokines via activation of NF-κB in endothelial cells. *FASEB J Sep.* 2016;30(9):3097–106. <https://doi.org/10.1096/fj.201600368RR>.
29. Kern F, Kuhn T, Ludwig N, Simon M, Gröger L, Fabis N, Aparicio-Puerta E, Salhab A, Fehlmann T, Hahn O, Engel A, Wagner V, Koch M, Winek K, Soreq H, Nazarenko I, Fuhrmann G, Wyss-Coray T, Meese E, Keller V, Laschke MW, Keller A. Ageing-associated small RNA cargo of extracellular vesicles. *RNA Biol Jan.* 2023;20(1):482–94. <https://doi.org/10.1080/15476286.2023.2234713>.
30. Ling M, Tang C, Yang X, Yu N, Song Y, Ding W, Sun Y, Yan R, Wang S, Li X, Gao H, Zhang Z, Xing Y. Integrated metabolomics and phosphoproteomics reveal the protective role of exosomes from human umbilical cord mesenchymal stem cells in naturally aging mouse livers. *Exp Cell Res. Jun* 1;427(1):113566, 2023. <https://doi.org/10.1016/j.yexcr.2023.113566>
31. Gomez I, Ward B, Souilhol C, Recarti C, Ariaans M, Johnston J, Burnett A, Mahmoud M, Luong LA, West L, Long M, Parry S, Woods R, Hulston C, Benedikter B, Niespolo C, Bazaz R, Francis S, Kiss-Toth E, van Zandvoort M, Schober A, Hellewell P, Evans PC, Ridger V. Neutrophil microvesicles drive atherosclerosis by delivering miR-155 to Atheroprone endothelium. *Nat Commun Jan.* 2020;10(1):214. <https://doi.org/10.1038/s41467-019-14043-y>.
32. Lee S, Lee HC, Kwon YW, Lee SE, Cho Y, Kim J, Lee S, Kim JY, Lee J, Yang HM, Mook-Jung I, Nam KY, Chung J, Lazar MA, Kim HS. Adenylate cyclase-associated protein 1 is a receptor for human resistin and mediates inflammatory actions of human monocytes. *Cell Metab.* Mar 4;19(3):484–97, 2014. <https://doi.org/10.1016/j.cmet.2014.01.013>
33. Munjas J, Sopić M, Spasojević-Kalimanovska V, Kalimanovska-Oštrić D, Anđelković K, Jelić-Ivanović Z. Association of adenylate cyclase-associated protein 1 with coronary artery disease. *Eur J Clin Invest Sep.* 2017;47(9):659–66. <https://doi.org/10.1111/eci.12787>.
34. Zhou L, Li JY, He PP, Yu XH, Tang CK, Resistin. Potential biomarker and therapeutic target in atherosclerosis. *Clin Chim Acta Jan.* 2021;512:84–91. <https://doi.org/10.1016/j.cca.2020.11.010>.
35. Hua K, Li T, He Y, Guan A, Chen L, Gao Y, Xu Q, Wang H, Luo R, Zhao L, Jin H. Resistin secreted by Porcine alveolar macrophages leads to endothelial cell dysfunction during haemophilus parvus infection. *Virulence.* Dec; 2023;14(1):2171636. <https://doi.org/10.1080/21505594.2023.2171636>.

## Publisher's note

Springer Nature remains neutral with regard to jurisdictional claims in published maps and institutional affiliations.